AWARD NUMBER: W81XWH-22-1-0679

TITLE: Vascular Organoids to Model Inherited Vascular Diseases

PRINCIPAL INVESTIGATOR: Dr. Maria Trivieri, MD, PhD

CONTRACTING ORGANIZATION: Icahn School of Medicine

REPORT DATE: SEPTEMBER 2023

TYPE OF REPORT: ANNUAL

PREPARED FOR: U.S. Army Medical Research and Development Command
Fort Detrick, Maryland 21702-5012

REPORT DOCUMENTATION PAGE

Form Approved
OMB No. 0704-0188

1. REPORT DATE	**2. REPORT TYPE**	**3. DATES COVERED** *(From - To)*
SEPTEMBER 2023	ANNUAL	15AUG2022 - 14AUG2023

4. TITLE AND SUBTITLE

Vascular Organoids to Model Inherited Vascular Diseases

5a. CONTRACT NUMBER

W81XWH-22-1-0679

5b. GRANT NUMBER

5c. PROGRAM ELEMENT NUMBER

6. AUTHOR(S)

Dr. Maria Trivieri, MD, PhD

E-Mail:mariagiovanna.trivieri@mountsinai.org

5d. PROJECT NUMBER

5e. TASK NUMBER

5f. WORK UNIT NUMBER

7. PERFORMING ORGANIZATION NAME(S) AND ADDRESS(ES)

AND ADDRESS(ES)

Icahn School of Medicine

Department of Medicine - Cardiology One
Gustave L. Levy Place
New York, NY 10029-6574

8. PERFORMING ORGANIZATION REPORT NUMBER

9. SPONSORING / MONITORING AGENCY NAME(S) AND ADDRESS(ES)

U.S. Army Medical Research and Development Command

Fort Detrick, Maryland 21702-5012

10. SPONSOR/MONITOR'S ACRONYM(S)

11. SPONSOR/MONITOR'S REPORT NUMBER(S)

12. DISTRIBUTION / AVAILABILITY STATEMENT

Approved for Public Release; Distribution Unlimited

13. SUPPLEMENTARY NOTES

14. ABSTRACT

Hereditary Hemorrhagic Telangiectasia (HHT) is a debilitating condition characterized by vascular malformations and pulmonary hypertension (PH). Mutations in the ALK1 gene are a major cause of HHT-associated PH, but the underlying cellular and molecular mechanisms are poorly understood. To address this knowledge gap, this proposal aims to generate biomimetic vascular organoids from induced pluripotent stem cells (iPSCs) harboring two common ALK1 mutations. These organoids could provide a more realistic and physiologically relevant platform for studying the process of vascular remodeling (VAR) in HHT-associated PH. This information could lead to the development of new therapeutic strategies for this devastating disease.

15. SUBJECT TERMS

NONE LISTED

16. SECURITY CLASSIFICATION OF:			**17. LIMITATION OF ABSTRACT**	**18. NUMBER OF PAGES**	**19a. NAME OF RESPONSIBLE PERSON**
					USAMRDC
a. REPORT	**b. ABSTRACT**	**c. THIS PAGE**	UU	17	**19b. TELEPHONE NUMBER** *(include area code)*
U	U	U			

Standard Form 298 (Rev. 8-98)
Prescribed by ANSI Std. Z39.18

TABLE OF CONTENTS

1. INTRODUCTION

Hereditary Hemorrhagic Telangiectasia (HHT) is an inherited condition characterized by vascular malformations in various body organs, particularly the lungs, liver, and brain. Patients affected by this disease generally present with chronic, severe bleeding necessitating frequent blood transfusion and/or pulmonary hypertension (PH). The latter is a devastating disease, with a very poor prognosis, characterized by the narrowing of the artery leading from the heart to the lungs that results in an elevation in pressure. If left untreated, this cardiopulmonary condition can lead to failure of the right heart and premature death. Dysfunction of the cells that constitute the blood vessels, such as Endothelial Cells (EC) and smooth muscle cells (SMC), has been implicated in the process of vascular remodeling (VAR) commonly seen in this condition. Mutations in the activin receptor-like kinase 1 *ALK1* gene resulting in haploinsufficiency are among the underlying culprits for the vascular abnormalities seen in HHT and associated PH. Carriers of this mutation typically develop PH earlier than carriers of other mutations linked to inherited PH and have a more severe course. Because neither the cellular nor the molecular programs that orchestrate this process have been fully elucidated, the mainstream treatment is supportive care with transfusion for chronic bleeding and vasodilatory therapy for PH. To address this knowledge gap, the proposal is centered on characterizing induced pluripotent stem cells (iPSC) harboring two common *ALK1* mutations. Using these hiPSCs, the plan is to generate biomimetic vascular organoids. These complex three-dimensional organ-like model systems are believed to more faithfully recapitulate the complexity of the human organ and provide a more realistic physiological platform due to the molecular similarity to their tissue of origin. Organoids have been generated for various organs, including the liver and lungs. More recently, they have been used to model diabetic vasculopathy4. The goal is to leverage this system to create human-specific organoid models that could recapitulate the process of VAR seen in *ALK1*-related HHT and PH.

2. KEYWORDS

Hereditary Hemorrhagic Telangiectasia; Pulmonary Hypertension; Vascular Organoids; 3D vascular Organoids

3. ACCOMPLISHMENTS

The overall goal of this project is to elucidate the mechanisms regulating *ALK1*-dependent modulation of VAR, discover new druggable pathways, and offer a valuable platform for the characterization of the *ALK1* as well as other mutations involved in HHT and PH or for pre-clinical drug testing. To achieve these objectives,

a complex series of experiments have been devised that involve the characterization of *ALK1* Mutant 3D Vascular Organoids both in vitro and in vivo. Specifically, our plan involved the:

- Generation of *ALK1* mutant hiPSCs using CRIPSR gene editing followed by validation steps that include testing for pluripotency and genomic stability.
- Differentiation and characterization of control hiPSCs into ECs.
- Differentiation and characterization of *ALK1* mutant hiPSCs into ECs.
- Differentiation and characterization of hiPSCs-derived self-assembled 3D vascular organoids generated from *ALK1* mutant cell lines.

More specifically:

a. *ALK1* mutant hiPSCs characterization including CRISPR based gene editing and validation.

In this first subsection, we describe our comprehensive assessment of the *ALK1* mutant hiPSCs, following CRISPR-mediated gene editing. Figure 1 serves as a visual aid to encapsulate our findings. Panel A depicts the details of the *ALK1* CRISPR-induced mutations. Sanger sequences were aligned and compared to the original sequence of the hiPSC cell line used for editing (Fig.1 A). The comparison showed the DNA sequence of three distinct and novel cell lines, namely Clone 34, Clone 15.4, and Clone 7, providing unequivocal evidence of the genetic mutation we have introduced.

Utilizing Sanger sequencing, we assessed the extent of knock-in and knockout modifications in our cell lines with the assistance of the "*Inference of CRISPR Edits (ICE, Synthego) algorithm*". ICE provided valuable insights into the characterization of the three cell lines. Specifically, Clone 34 (KD1) demonstrated successful heterozygous knock-in modification, with an Indel percentage of 60 and KI-Score of 60, validating the accuracy of the genetic modification. Clone 15.4 (KD2) exhibited a highly successful homozygous knock-in mutation, with an Indel percentage of 99 and an outstanding KI-Score of 99, indicating a robust genetic alteration. For Clone 7 (KO), our analysis suggested a likely functional knockout, with an Indel percentage of 94 and a KO-Score of 94, implying a significant disruption of the target gene.

The three clones were subjected to a Global Diversity Array with Cytogenetics (GDA-Cyto) to verify whether the karyotype was unaltered after editing (Fig1.B) In Fig.1, panel B, we present a representative Normal karyotype for the *ALK1* knockout Clone 7 (KO). All three clones were considered normal, with no copy number variations (CNVs) higher than 1.5 Mb detected and no absence of heterozygosity (AOH). This critical step confirmed the success of our genetic modification and cell lines' generation without any genetic

aberration. Panel C includes representative images validating the pluripotency of our cell lines. Specifically, it contains representative images of immunofluorescence staining using the pluripotency markers OCT4 (in red) and SSEA4 (in green) in a wild-type (CTRL) cell and the other three remaining mutant lines (CT1, KD1, KD2, and KO). Panel D displays representative images of immunofluorescence with markers such as SOX2 (in yellow) and TRA-1-60 (in magenta) in all four cell lines (CT1, KD1, KD2, and KO). Together, Figs. 1C and D demonstrated the expression of the four relevant pluripotency markers across all cell lines, reinforcing the quality of our cell preparations for further experimentation.

In summary, the data presented above confirms robust expression of pluripotency markers and successful CRISPR gene editing. Collectively, these findings firmly demonstrate that our *ALK1* hiPSC lines are appropriate for the subsequent phases of our research study, which will include functional and more in-depth transcriptomic characterization.

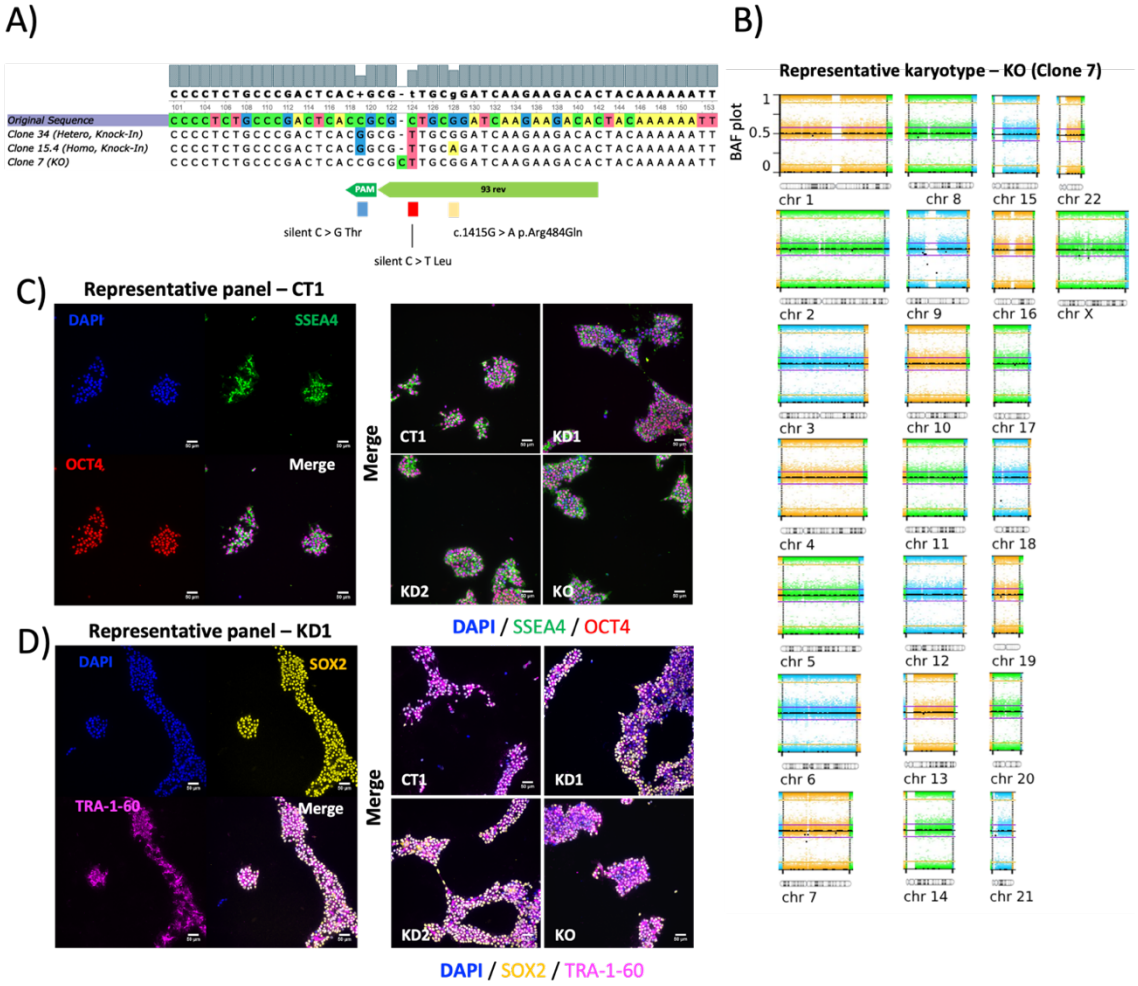

Figure 1: *ALK1 mutant hiPSCs CRISPR gene editing, expression of pluripotency markers, and genomic stability*. A) Aligned sequences showing the CRISPR-induced mutations in the hiPSC (wildtype – "Original sequence") cell line, the original sequence, heterozygote Knock-In, homozygote Knock-In, and Knockout cell lines. B) Representative Karyotype for the *ALK1* KO clone 7. The three clones underwent a Global Diversity Array with Cytogenetics (GDA-Cyto). BAF plots are presented with Chromosome maps. C) Representative images of immunofluorescence staining with OCT4 (red) and SSEA4 (green) markers for a wild-type (CTRL) cell and the remaining lines (CT1, KD1, KD2, and KO). D) Representative images of immunofluorescence reaction against SOX2 (yellow) and TRA-1-60 (magenta) from a Knock-In cell (Hetero) and merged images of these pluripotency markers for all four cell lines (CT1, KD1, KD2, and KO). All the hiPSC-colonies display the expression of the pluripotency markers, confirming that the cells are adequate for the next steps of this study. Cells were passaged at 80% confluence using VERSENE (non-enzymatic method) in a 1:10 density ratio. Cells were kept in mTeSR plus for 48h after seeding and then fixed with 4% PFA.

b. Differentiation of hiPSCs into endothelial cells

Next, we demonstrated the establishment of a successful protocol for the differentiation of human induced pluripotent stem cells (hiPSCs) into endothelial cells (ECs), an essential step for this project. Figure 2 serves as our visual guide to illustrate the various steps.

In Panel A, we present a step-by-step schematic pictorial of the different stages of the differentiation process, starting from the seeding of hiPSCs followed by the timed addition of specific growth factors. The protocol culminates on Day 20 when cells were primed for the immunohistochemical characterization. Fig. 2B (Day 20): transmitted light (TL) images of hiPSC-ECs revealed their distinct cellular morphology compared to hiPSCs and their similarity with HUVEC cells (bottom right). No differences were observed when the initial cell densities were varied at Day 0 (20, 40, and 60x10ˆ3/cm2). By Day 5, the impact of initial seeding (data not shown) on cell morphology was more apparent. Notably, the yield of VE-Cadherin-positive cells remained consistently high, exceeding 90% across all tested cell densities (data not shown). For the subsequent analyses, the lowest initial cell density of 20x10ˆ3 cell/cm2 was used (Fig. 2C-F).

In Fig.2C, we showed immunofluorescence (IF) images at 20X magnification of hiPSC-ECs. DAPI staining (blue) highlights cell nuclei, while VE-Cadherin (green) and CD31 (yellow) demonstrate their endothelial cell identity. In addition, the inner cellular structure was very clearly outlined by F-actin staining (red, phalloidin-PHA). These images prove that we can successfully differentiate hiPSCs into endothelial-like cells. Furthermore, we were able to image and quantify VE-Cadherin positive hiPSC-ECs from two independent batches of differentiation (Fig.2D). Image segmentation and analysis underscore the consistency of VE-Cadherin expression and the robustness of our differentiation protocol (95.22% and 96.57% VE-Cadherin positive cells on differentiations 1 and 2, respectively).

To test the functional properties of hiPSC-ECs, we conducted two routine endothelial cell assays on Day 20. In Fig. 2E, the 2D Tube Formation assay showcased the ability to form tube-like structures after 24 hours of incubation. Remarkably, cells cultured in EGM-2 medium supplemented with VEGFA displayed sustained tube formation, confirming their functional competence. Even when grown in less favorable conditions, such as the essential MEM media, our cells demonstrated endothelial-like behavior in culture (Fig. 2E, upper panel). Lastly, Panel F demonstrates the results of the LDL uptake assay in CT1 hiPSC-ECs. After exposure to LDL-Dylight™ 550, cells were fixed and stained for LDL receptor (LDLR) and CD31 proteins. The

images demonstrate the uptake of LDL (in red) and expression of LDLR (in green), further validating the functionality of hiPSC-ECs.

In conclusion, our results offer evidence of a successful differentiation of hiPSCs into endothelial cells. These hiPSC-EC express the appropriate cellular markers, have the ability to form tubes, and uptake LDL highlighting the success of this pivotal part of the project.

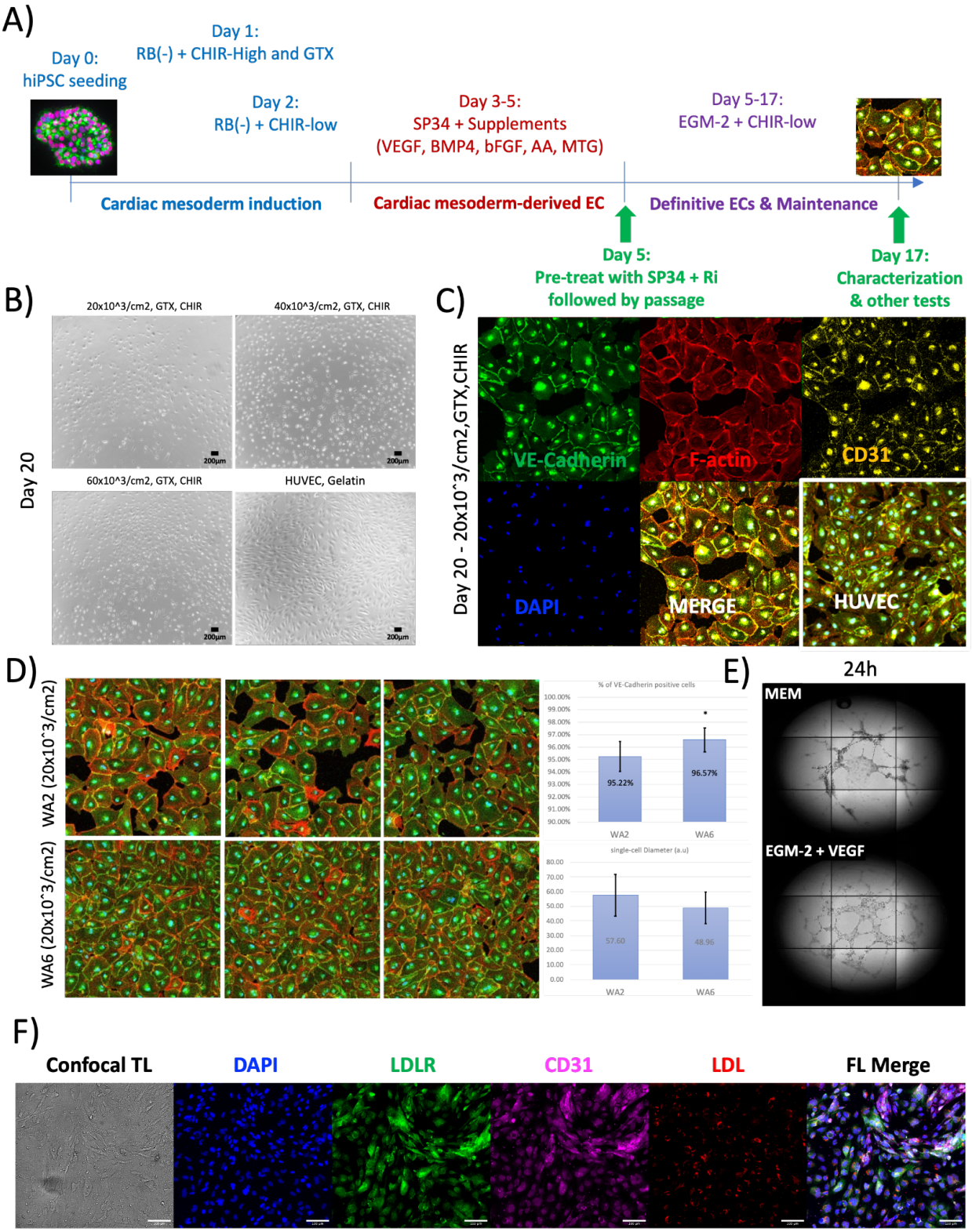

Figure 2: *Differentiation and characterization of hiPSCs into endothelial cells.* A) Schematic representation of the differentiation of cardiac mesoderm-derived endothelial cells from human induced pluripotent stem cells (hiPSCs). On day 0, hiPSCs were seeded at 2.5x10ˆ4 cells/cm2 and cultured for 24h in mTeSR. On day 1, mTeSR was replaced with RPMI supplemented with B27 minus insulin (RB(-)) and CHIR99021 (6μM, CHIR-High) and 1:60 of GelTrex (GTX), which induced cells to differentiate into cardiac mesoderm. On day 2, the cells were treated with RB(-) supplemented with CHIR99021 (2μM, CHIR-low) for 16h, further promoting their differentiation into cardiac mesoderm. On days 3-5, the cells were cultured in StemPro 34 medium supplemented with VEGF, BMP4, bFGF, ascorbic acid, and 1-Thioglycerol (MTG). On day 5, the cells were pre-treated with Rock inhibitor (y-27632) for 2h, followed by a passage at 0.9x10ˆ4 cells/cm2 density. Cells were then cultivated in EGM-2 medium supplemented with 2μM of CHIR99021, and the media was changed daily. On day 17, the cells were passaged for immunohistochemical characterization. Cells were kept in EGM-2 without CHIR supplementation for 72h and then fixed for immunofluorescence reactions (Day 20 hiPSC-ECs). B) Transmitted light (TL) images of hiPSC-ECs. The images in B are from Day 20 cells, which had undergone splitting on Day 5 and were subsequently seeded with similar densities. On Day 5, distinct densities were observed for each condition tested. C) Immunofluorescence (IF) images of hiPSC-ECs. 20X magnification. In blue: DAPI, in green: VE-Cadherin, in red: F-actin (phalloidin-PHA), and in yellow: CD31. D) Two independent batches of diff. and VE-Cadherin quantification. 20X magnification. In blue: DAPI, in green: VE-Cadherin, and in red: F-actin (phalloidin-PHA). The percentage of VE-Cadherin-positive cells was significantly different compared to the two independent batches ($P<0.05$). On both, the percentage of positive cells was higher than 95%. The long-axis diameter of hiPSC-ECs from bot batches was similar ($P>0.05$). Images were segmented using the Python version of Cellpose (cellpose.org), and cell morphometrics and percentages were calculated using custom scripts and algorithms (based on Blobs Analysis) crafted in MATLAB. E) Representative images of the 2D Tube Formation assay after 24h of incubation. Cells were seeded onto 96-well plates pre-treated with 30 μL of GelTrex (12-18 mg/mL) and kept in MEM or EGM-2 supplemented with 300ng/mL of VEGFA. Images were taken from the whole well in stitches with 10% overlapping. The stitches were combined using ImageJ>Plugins>Stitching>Grid/collection stitching. Note the tube-like formations on the EGM-2 sample and compare them with the MEM control. EGM-2 media supplemented with VEGFA resulted in a more robust and morphologically compelling tube formation. F) Representative images of the LDL uptake assay in wild-type hiPSC-ECs. Day 17 hiPSC-ECs cells were cultured at a density of 3 x 10ˆ4 cells/well in a 96 well plate for three days; then LDL-DylightTM 550 (10μg/ml) was added, and the cells were incubated for four hours. Cells were fixed (Day 20) and stained for LDL receptor using a Rabbit anti-LDL receptor primary antibody Dylight™ 488-conjugated secondary antibody, and CD31. 20X magnification. Scale bar: 100um. In blue: DAPI, in green: LDLR, in red: LDL (uptake), and in magenta: CD31.

c. *ALK1* mutant hiPSCs differentiation into endothelial cells - pilot experiments

In Figure 3, we explored the differentiation of *ALK1* mutant hiPSCs into endothelial cells. Fig.3A serves as the roadmap, outlining the steps of this differentiation process. From the initial seeding of hiPSCs to the final immunohistochemical characterization on Day 20, we followed the same steps shown in the previous section.

In Fig.3 (B to D), we show representative immunofluorescence images targeting VE-Cadherin, a cell surface marker specific and exclusive for endothelial cells. Four distinct cell lines - wild-type control (CT1), *ALK1* mutant heterozygote (KD1), *ALK1* mutant homozygote (KD2), and *ALK1* Knock-out (KO) – were differentiated in parallel, in three independent batches (Diff.1, Diff.2, and Diff.3). The images, captured at 20X magnification, revealed the expression of VE-Cadherin (in green), highlighting the endothelial identity of these cells. Qualitatively, up to 90-95% of cells were stained for VE-Cadherin across all preparations. The VE-Cadherin antibody was validated in HUVEC cells to ensure its specificity. We also included a negative control using hiPSCs (data not shown). In summary, Figure 3 offers a visually captivating demonstration of our ability

to differentiate *ALK1* mutant hiPSCs into ECs with the emergence of a high percentage of VE-Cadherin positive cells, emphasizing the successful transformation of these cells into an endothelial-like phenotype. We are currently working on a more in-depth morphological, molecular, and functional characterization of these cell lines to understand the impact of *ALK1* mutations on endothelial cell behavior.

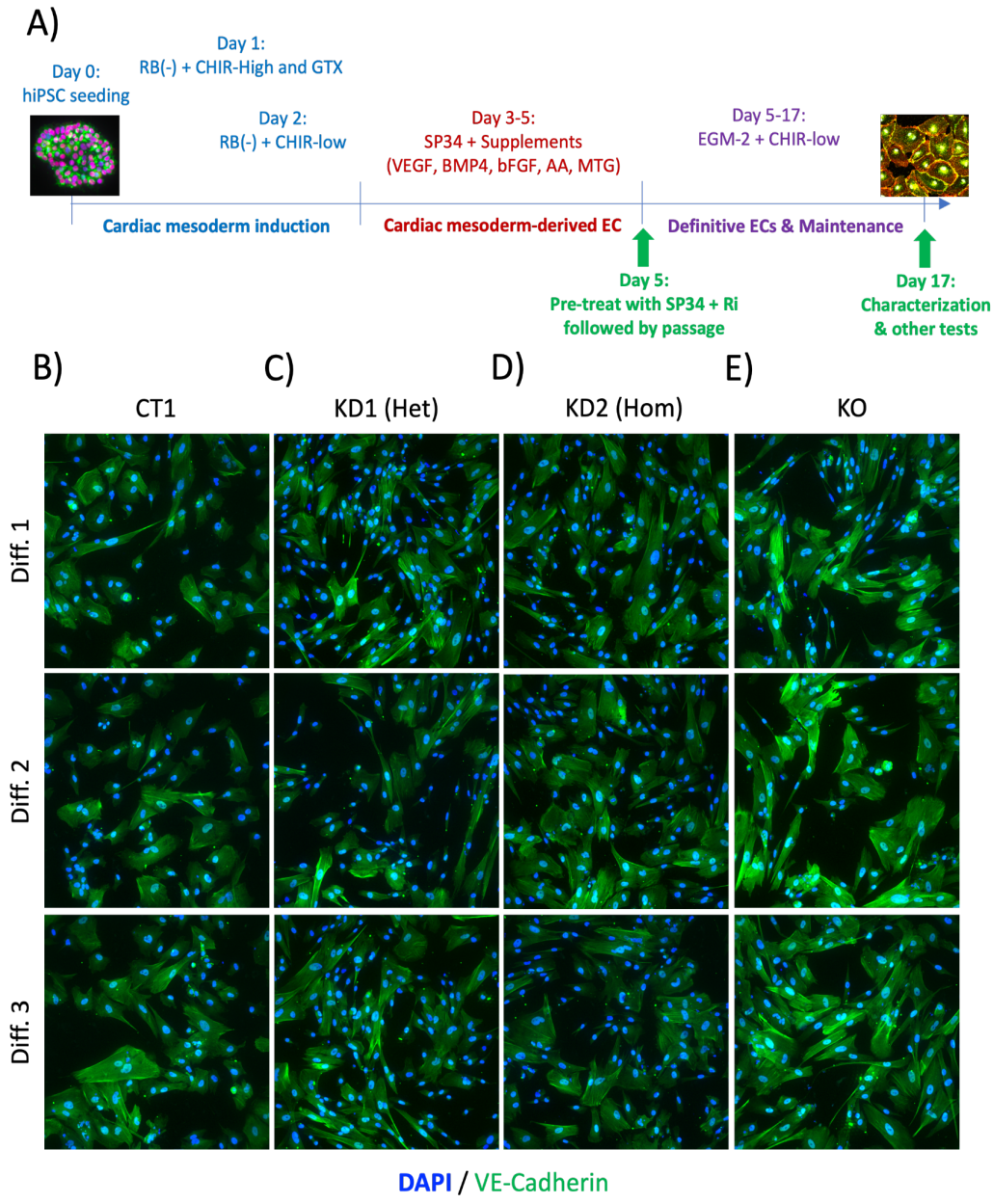

Figure 3: *ALK1 mutant hiPSCs differentiation into endothelial cells.* A) Schematic representation of the differentiation of cardiac mesoderm-derived endothelial cells from human induced pluripotent stem cells (hiPSCs). On day 0, hiPSCs were seeded at 2.5x10^4 cells/cm2 and cultured for 24h in mTeSR. On day 1, mTeSR was replaced with RPMI supplemented with B27 minus insulin (RB(-)) and CHIR99021 (6μM, CHIR-High) and 1:60 of GelTrex (GTX), which induced the cells to differentiate into cardiac mesoderm. On day 2, the cells were treated with RB(-) supplemented with CHIR99021 (2μM, CHIR-low) for 16h, further promoting their differentiation into cardiac mesoderm. On days 3-5, the cells were cultured in StemPro 34 medium supplemented with VEGF, BMP4, bFGF, ascorbic acid, and 1-Thioglycerol (MTG). On day 5, the cells were pre-treated with Rock inhibitor (y-27632) for two hours, followed by passage. After passage, cells were cultivated in the EGM-2 medium supplemented with 2μM of CHIR99021 with daily media changes. On day 17, the cells were passaged for immunohistochemical characterization. Cells were kept in EGM-2 without CHIR supplementation for 72h and then fixed for immunofluorescence reactions (Day 20 hiPSC-ECs). B-D) Representative images of Immunofluorescence reactions against VE-Cadherin, an exclusive marker of endothelial cells. Four cell lines (wildtype control – CT1, *ALK1*-mutant c.1451G > A p.Arg484Gln in heterozygosis - KD1 (Het), *ALK1*-mutant c.1451G > A p.Arg484Gln in homozygosis – KD2 (Hom), and *ALK1* Knock-out, KO, respectively) were differentiated in parallel, three independent times (Diffs. 1, 2 and 3) and characterized on day 20 by immunofluorescence reaction. In green, VE-Cadherin, in blue DAPI. These images were captured using a 20X magnification lens. Five stacks of 2um were piled to generate a maximum intensity projection (MIP). Qualitatively, we estimate that up to 90-95% of cells were positive for VE-Cadherin. The VE-Cadherin antibody was previously validated in HUVEC and a negative control using hiPSCs was also used. On day 17, 2x10^4 cells/cm2 were seeded in each well of a 96-well plate.

d. Differentiation and preliminary characterization of hiPSC-derived self-assembled 3D vascular organoids

In this section, we describe the differentiation and preliminary characterization of hiPSC-derived self-assembled 3D vascular organoids obtained through four distinct protocols. The results presented in this section were obtained using wild-type (CT1) cells and will be subsequently repeated in the three mutant lines.

In Fig. 4A, we outline the differentiation process using a schematic encompassing four distinct protocols (Prot. 1, Prot. 2, Prot. 3, and Prot. 4, as detailed in Table 1). These protocols were meticulously designed to facilitate the transition from a 2D environment to a 3D culturing system. To achieve this, we recalibrated the concentration of the small molecules and recombinant proteins in the culture media to promote the 3D differentiation of hiPSCs into vascular organoids. Specifically, we devised Stoichiometric protocols (Prot. 2 and 4) tailored to the number of cells required for the generation of the 3D spheres in relation to the volume capacity of the 96-well plates. Prot. 1 and 3, which utilized standard small molecules used for 2D concentrations without considering cell numbers and media volumes. Additionally, Prot. 1 and 2 incorporated EGM-2 supplementation with 2μM CHIR99021 after day 5, while Prot. 3 and 4 organoids remained submerged exclusively in EGM-2 media. Starting from the seeding of 5000 hiPSCs in an ultra-low attachment plate, day 1 marked the transition to RPMI supplemented with CHIR99021, initiating the process of mesodermal differentiation. Day 2 sees a shift to CHIR99021 with a focus on vascular mesoderm, while days 3-5 involve culture in StemPro 34 medium enriched with various factors (Table 1). By day 5, we introduce EGM-2 medium was introduced, with or without CHIR99021, depending on the protocol. On day 11, the respective vascular organoids were fixed and characterized by immunohistochemistry.

Table 1: Media Composition According to Various Protocols:

Protocol	Day 1	Day 2	Day 3-5	Day 5-11
Prot. 1	6µM CHIR	2µM CHIR	300ng/mL VEGF, 10ng/mL BMP4, 5ng/mL bFGF	2µM CHIR
Prot. 2	7.66µM CHIR	2.55µM CHIR	33.3ng/mL VEGF, 1.1ng/mL BMP4, 0.54ng/mL bFGF	2µM CHIR
Prot. 3	6µM CHIR	2µMCHIR	300ng/mL VEGF, 10ng/mL BMP4, 5ng/mL bFGF	NO CHIR
Prot. 4	7.66µM CHIR	2.55µM CHIR	33.3ng/mL VEGF, 1.1ng/mL BMP4, 0.54ng/mL bFGF	NO CHIR

In Fig.4, Panel B, transmitted light images of the vascular organoids cultivated using the four different protocols over the course of 11 days were represented. These 10X magnification images were crafted from the Z-stack series, providing a glimpse into their growth and complexity over a very short period of experimentation. Quantitative insights into their growth kinetics regarding area and circularity are displayed in Fig.4C and D. These metrics offer a deeper understanding of the morphological changes occurring within these 3D vascular organoids and reveal distinct patterns.

From Day 0 to Day 3, there was no difference in the area occupied by each organoid, independently of the protocol used. However, on day 3, Prot. 1 and 3 organoids showed significantly lower circularity than Prot. 2 and 4 (the stoichiometric, $P<0.05$). After day 5, Prot. 1 and 2 included daily treatment with EGM-2 supplemented with 2µM of CHIR99021. On day 11, these treatments affected the area of the organoids, with a significant increase in the area for Prot. 1, 2, and 4 compared to Prot. 3 (Fig.4C). Also, the circularity was significantly impacted, denoting morphological changes in the organoids generated using CHIR99021 after day 5 (Prot. 1 and 2, Fig.4D). Organoids treated with CHIR99021 after day 5 displayed long tubular-like protrusions coming from the spheric portions, whereas the non-CHIR protocols resulted in very small and round organoid, without protrusion (Fig.4D, E and F). Curiously, Prot. 4 organoids were larger than their pairwise comparison (Prot. 3, day 5 CHIR vs. Non-CHIR comparison, Fig.4C).

In Fig.4E, we explored with immunofluorescence images captured at 10X magnification from Z-stack series, the intricacies of each organoid generated by the different protocols. DAPI staining (blue) reveals cell nuclei, while CD31 (green) highlights vascular structures, and phalloidin (PHA, red) outlines cell structures. In line with what we observed using light microscopy, Prot. 1 and 2 organoids displayed more intricated

morphology (Fig.4E, two upper panels). A CD31-positive cells well-established network was observed in all the organoids, always in the spheric portion of these organoids (Fig.4F, yellow and purple asterisks - left panels). Within the part that was protruding, a very organized and tubular structure was instead observed (Fig.4F, white dashed lines and asterisks). For both, Prot. 1 and Prot. 2, long and thin endothelial cells (CD31-positive) were observed in the inner walls of the tubules (Fig.4E and F). Despite the roundness of the organoids generated with Prot. 3 and 4, small tubules were also observed in their core mass (Fig.4F, lower right). Interestingly, all tubules, small and large, were covered by a very peculiar cell type with a cuboidal to columnar morphology, resembling simple cuboidal and simple columnar epithelial cells (Fig.4F, yellow and blue arrows, respectively).

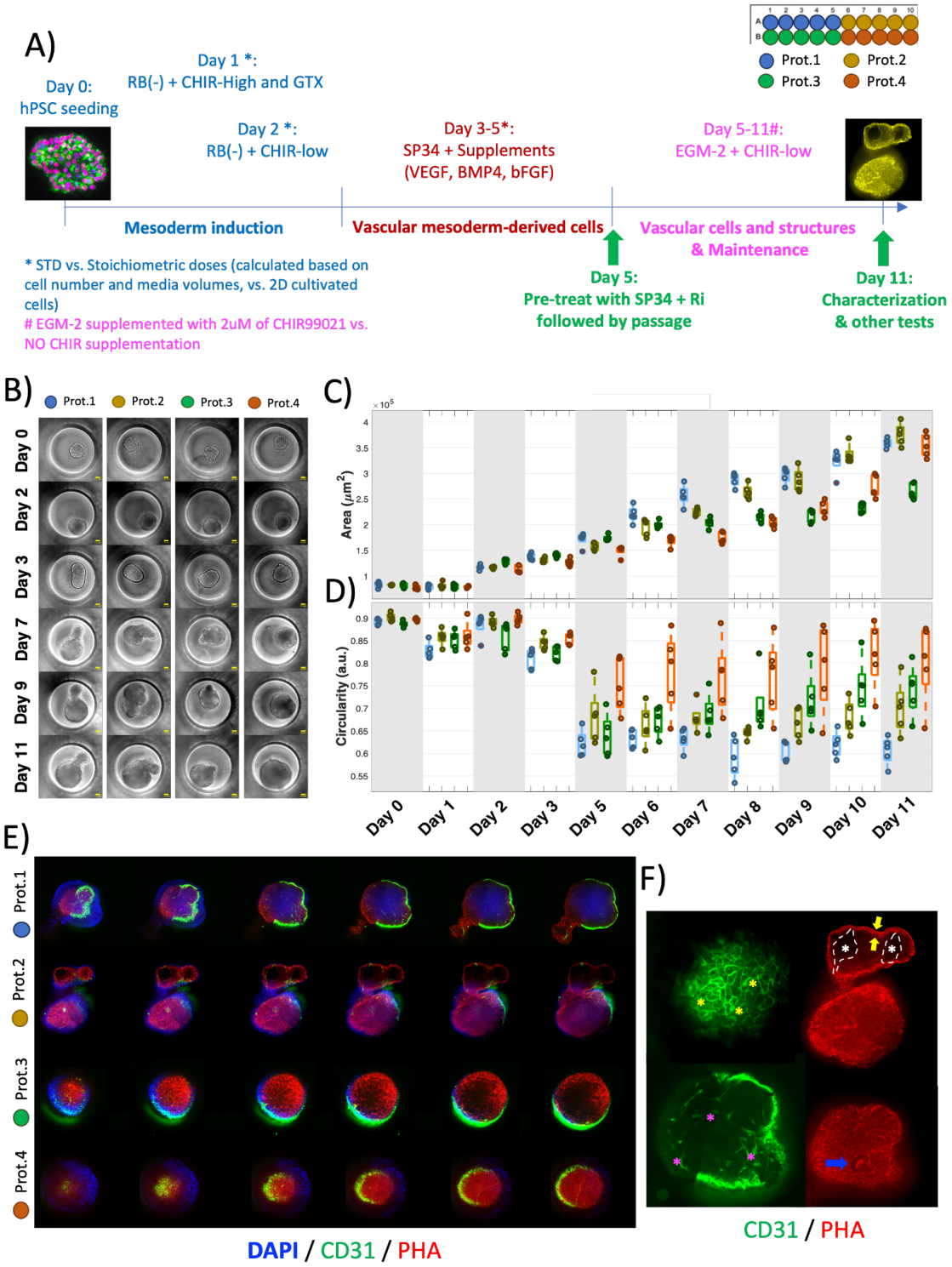

In sum, Figure 4 unravels the differentiation and early characterization of hiPSC-derived 3D vascular organoids. It offers a vivid glimpse into their growth, complexity, and intricate structures, setting the stage for further exploration and understanding.

Figure 4: *Differentiation and preliminary characterization of hiPSCs-derived self-assembled 3D vascular organoids.* A) Schematic representation of the differentiation of hiPSC-derived self-assembled 3D vascular organoids by four protocols. On day 0, 5000 hiPSCs were seeded and cultured for 24h in mTeSR plus y-27632 (Rock inhibitor, 10μM) in an ultra-low attachment, flat bottom, 96-wells plate. On day 1, mTeSR was replaced with RPMI supplemented with B27 minus insulin (RB(-)) and CHIR99021 (6μM-Prots. 1 and 3 or 7.66μM-Prots. 2 and 4, CHIR-High), which induced the cells to differentiate into mesoderm. On day 2, the cells were treated with RB(-) supplemented with CHIR99021 (2μM-Prots. 1 and 3 or 2.55μM-Prots. 2 and 4, CHIR-low) for 16h, which further promotes their differentiation into cardiovascular mesoderm. On days 3-5, the cells were cultured in StemPro 34 medium supplemented with VEGF, BMP4, bFGF, ascorbic acid, and 1-Thioglycerol (MTG). Protocols 2 and 4, contained 9X less of the aforementioned molecules (check Table 1). From day 5, cells were cultivated in EGM-2 medium supplemented with or without supplementation of 2μM of CHIR99021 (Prots. 1 and 2 vs. Prots. 3 and 4, respectively), with daily media changes. On day 11, vascular organoids were subjected to fixation with 4% PFA and further immunohistochemical characterization. B) Transmitted light images of vascular organoids generated using four different protocols over an 11-day period. 10X magnification, Maximum intensity projection, Z-stack series of 5 images with 25-30μm per slice. C) 3D vascular organoids quantification of growth kinetics – Area/Size. Images were segmented using the Python version of Cellpose (cellpose.org), and cell morphometrics and percentages were calculated using custom scripts and algorithms (based on Blobs Analysis) crafted in MATLAB. D) 3D vascular organoids growth kinetics quantification – Circularity/Complexity. Images were segmented using the Python version of Cellpose (cellpose.org), and cell morphometrics and percentages were calculated using custom scripts and algorithms (based on Blobs Analysis) crafted in MATLAB. E) Immunofluorescence images of vascular organoids generated using four different protocols over an 11-day experiment. 10X magnification, Maximum intensity projection, Z-stack series of 8 images with 25-30μm per slice. In blue: DAPI, in green: CD31, in red: phalloidin (PHA). F) Representative images of relevant structures in the 3D vascular organoids originated using wild-type hiPSCs. Yellow asterisks: an intricated layer of CD-31 positive cells. Magenta asterisks: “relaxed” network structure of CD-31 positive cells connected to the “core” of the vascular organoid. White asterisk: “vessel-like” lumen. White dashed line: “vessel-like” inner wall covered by CD31-positive cells (green). Yellow arrows: simple cuboidal epithelial cells? Blue arrow: simple columnar epithelial cells?

e. Opportunities for training and professional development until this stage

Our project focuses on advancing CRISPR gene editing and iPSC differentiation into EC and Vascular Organoids. We have prioritized comprehensive training and professional development for all project participants, including the Principal Investigator (PI) and the Postdoctoral Fellows.

At this project stage, the PI and the Postdoctoral Fellows have the unique opportunity to gain expertise in CRISPR gene editing and iPSC differentiation, which is essential in advancing scientific and medical innovation. Both the PI and the fellows are and will continue to receive hands-on training, collaborate with experts, and access cutting-edge resources to become specialists in these fields.

f. Plans for the next reporting period to accomplish our goals

We expect that with our next report, we will have completed a comprehensive analysis of the angiogenic properties of *ALK1* mutant hiPSC-derived endothelial cells and 3D vascular organoids both in vitro and in vivo. This includes transcriptomic analysis, spatial transcriptomics, functional assays, and pharmacological assessments using various drugs to mitigate the impact of the *ALK1* mutations on both, 2D and 3D models.

4. IMPACT

The proposed studies are highly innovative and will result in deeper understanding of the process of vascular arterial remodeling seen in carriers of the *ALK1* mutations manifesting with PH and HHT. In addition, the tools and methodology we are developing during the characterization of this model have the potential to be mirrored in other conditions, where a genetic mutation is identified, and its pathology could be readily characterized and similarly evaluated using vascular organoids. Indeed, if our approach is successful in recapitulating some of the features of this disease in a dish, there is the potential that it might be applied to other pathways and mutations, providing the premise for future "trials" in a dish. As such, beyond the investigation of the *ALK1* mutations, our proposal offers a flexible, innovative, and unique roadmap to guide the development of novel treatments for orphan cardiovascular inherited diseases.

5. CHANGES/PROBLEMS

Nothing to report.

6. PRODUCTS

Nothing to report.

7. PARTICIPANTS & OTHER COLLABORATING ORGANIZATIONS

Name	*Maria Giovanna Trivieri*
Project Role	*PI*
Researcher Identifier (e.g. ORCID ID)	*0000-0001-6601-3267*
Nearest person month worked	*2.4*
Contribution to Project	*Supervisor, Project Lead*
Funding Support	*This grant*
Name	*Antonio Fernando Ribeiro Junior*
Project Role	*Postdoctoral Fellow*
Researcher Identifier (e.g. ORCID ID)	*0000-0003-0373-9890*
Nearest person month worked	*6*
Contribution to Project	*Main researcher*
Funding Support	*This grant and other Institutional funds*

Name	*Rafael Dariolli*
Project Role	*Postdoctoral Fellow*
Researcher Identifier (e.g. ORCID ID)	*0000-0003-0957-1259*
Nearest person month worked	*8.4*
Contribution to Project	*Main researcher*
Funding Support	*This grant and other Institutional funds*

8. SPECIAL REPORTING REQUIREMENTS
Nothing to report.

9. APPENDICES
Nothing to report.